Synthesis and Characterization of Crystalline Graphene-Titania Nanocomposites as Efficient Photocatalysts for Pollution Control

K.M. Rajesh[1,*], S. Laxmi Priya[1], S. Rijith[2], K. Jithesh[3], V. Arun[4] and S. Sugunan[5]

[1]Post Graduate and Research Department of Chemistry, Sree Narayana College, Nattika-680566, India
[2]Post Graduate and Research Department of Chemistry, Sree Narayana College, Kollam-695101, India
[3]Post Graduate and Research Department of Chemistry, Sree Narayana College, Kannur-670007, India
[4]Post Graduate Department of Chemistry, Sree Narayana College, Punalur-691305, India
[5]Department of Applied Chemistry, Cochin University of Science and Technology, Cochin-682022, India

*Corresponding author: E-mail: rajeshkmamangalam@gmail.com

Titanium dioxide (TiO_2) is reported to exhibit high degradation efficiency to degrade organic water pollutants without any decomposition thereby acting as an excellent photocatalyst. The catalytic performance of pure TiO_2 (T1) can even be enhanced by incorporating graphene forming graphene-TiO_2 (GT1) nanocomposite. We suggest, a modified sol-gel method for synthesizing T1 and GT1 nanocomposites and they were characterized by XRD, FTIR, UV-visible spectra, TEM and XPS techniques. The removal efficiency of organic dye, methylene blue, was investigated by the photocatalytic degradation efficiency of GT1 nanocomposite under daylight irradiation. Degradation studies revealed that more than 90% methylene blue dye removal was achieved with 3 mg GT1 with an initial concentration of 10^{-4} M under an irradiation time of 1 h.

Keywords: Photocatalytic performance, Graphene-titania nanocomposite, Methylene blue dye, Pollution control.

INTRODUCTION

The frequent contamination of water sources by organic waste from various human activities makes water unfit for consumption and is also very hazardous for aquatic organisms [1,2]. For removing the carcinogenic organic pollutants from aquatic sources, several methods like coagulation, oxidation, ion exchange, adsorption, *etc.* are available, photocatalysis found to be more attractive due to its eco friendly nature and less toxic compounds formed by the degradation of organic dyes [3,4]. The nature of the adsorbent material selected for photocatalytic degradation of the dye is also very important. Different types of materials offers varying adsorption capacity and also their degradation efficiencies will also be different.

Nanotitania material can be effectively used for waste water treatment [5,6]. It offers enhanced stability, less hazardous nature and also economical. The highly oxidative holes in valence band of titania can react with organic pollutants generating OH radicals thereby achieving pollutant degradation [7]. However,

nanotitania also exhibits distinct drawbacks as it shows higher degradation activity only in UV-visible region and is less active in visible region of sunlight. Also the electron-hole pair recombination is higher in nanotitania [5,8-15].

Although various approaches are available for modifying titania [5,16-18]. We adopted a method by modifying nanotitania with reduced graphene oxide to overcome the disadvantages of titania [19-22]. Graphene offers high stability, better thermal conductivity, good electronic property, high surface area, mechanical strength, *etc.* [23-26]. Also graphene based nanocomposites provides catalytic efficiency, oxidising property and adsorbing ability, thereby making them excellent components for water purification. Thus, graphene incorporation in nanotitania can effectively enhance the quality of aquatic sources.

Due to its many applications in the medical, textile, and coir industries, the cationic dye methylene blue was chosen for this study of nanocomposite efficiency. Since methylene blue dye offers good solubility in alcohol and water, it is fre-

quently used in many pharmaceutical industries [27]. The increased concentration of methylene blue dye has the potential to provide a risk to the developing human fetus [28]. Hence, removal of methylene blue dye from aquatic sources is given the highest priority. Several attempt to degrade methylene blue dye was performed by various researchers by using different adsorbing materials [29,30]. Methylene blue dye degradation can be achieved by different methods such as electrochemical degradation, photocatalysis, electrocatalytic degradation, pulsed power technique, low temperature catalytic degradation, advanced oxidation process, *etc*. Among them, the photocatalytic degradation technique is more advantageous. Different materials like TiO_2, ZnO, WO_3, CdS, NiO, *etc*. are used for photocatalysis [31-38].

Several researchers have also reported the degradation of methylene blue dye using graphene-titania (TiO_2/GO) nanocomposites with varying degradation efficiency ranging from 60% to 100% [39-43]. However, the efficiency of degradation in a material is often closely linked to the manner in which it was produced. Even though several methods like *in situ* polymerization, hydrothermal, solvothermal, melt mixing, simple colloidal blending, self-assembly solution mixing, atomic layer deposition, electrospinning, aero-gel, sonochemical methods are available. We adopted sol-gel method since it allows the alteration of composition and microstructure by controlling precursor chemistry and processing conditions, resulting in the formation of a desired nanocomposite photocatalyst [7,18,19,28,44-48]. Additionally, the ultimate outcome provides a state of uniformity and integrity [49,50].

EXPERIMENTAL

Characterization: For XRD patterns, Bruker AXS D8 advance X-ray diffractometer was used and intensities were recorded. Thermo-Nicolet Avatar 370 spectrometer was used to obtain FTIR spectra. For recording diffuse reflectance UV-visible spectra, a Varian Cary 5000 UV-visible NIR spectrophotometer was employed. A Jeol JEM 2100 ultrahigh resolution electron microscope was used for obtaining the TEM images. For XPS results, an X-ray photoelectron microscope

with ESCA+ Omicron nanotechnology, Oxford Instrument, Germany was operated at 20 mA and 15 kV. The survey scan pass energy was 50 eV and short scan pass energy was 20 eV.

Synthesis of graphene oxide (GO1): For this, 9:1 H_2SO_4 and H_3PO_4 solutions were prepared. In a round bottom flask, 40 mL H_3PO_4 was added dropwise in to a flask containing 360 mL conc. H_2SO_4 and 3 g graphite powder with constant stirring. To this, 18 g $KMnO_4$ was added slowly, maintaining the temperature of mixture below 40 °C and stirred for 10 h. Later pour the mixture to 400 mL ice water along with 27 mL of 30% H_2O_2. Centrifuged the mixture and washed thoroughly with 1 M HCl and deionized water three times. Finally, it was filtered with 0.2 µ filter paper to obtain light brown powder [18,51,52].

Synthesis of reduced graphene oxide (RGO1): Prepared GO1 (100 g) was mixed with 100 mL of deionized water and sonicated for 90 min to obtain a yellow brown dispersion. This was then reduced to graphene by adding 1 mL hydrazine hydrate and the solution was heated for 14 h at 75 °C. It was then filtered, washed with ethanol, deionized water and obtained as a black solid.

Preparation of graphene-titania composite (GT1): A mixture of 0.08 g RGO1, 0.5 g cetyltrimethylammonium bromide (CTAB) and 25 mL ethanol was stirred magnetically for 30 min. To this, 11 mL titanium tetraisopropoxide and 20 mL deionized water were added, respectively dropwise. This was stirred for 8 h and dried at 60 °C to obtain a white gel, which was calcined at 500 °C for 10 min and finally cooled to room temperature. Pure titania was produced using the same method, but without the addition of RGO1.

RESULTS AND DISCUSSION

XRD analysis: In both Fig. 1a-b, prominent peaks were observed at 2θ = 25.5°, 38.1°, 48.2°, 54.3°, 55.1°, 62.9° which are attributed to (101), (004), (200), (105), (211) and (204) planes of anatase phase, respectively [5,18,53]. Also no peaks were observed at 2θ = 27.5° and 30.8°, which indicates the absence of rutile and brookite phases [6,54-56]. The size of crystallite calculated from 101 plane of anatase phase of GT1 and T1 were 8.85 nm and 9.2 nm, respectively. Also the cryst-
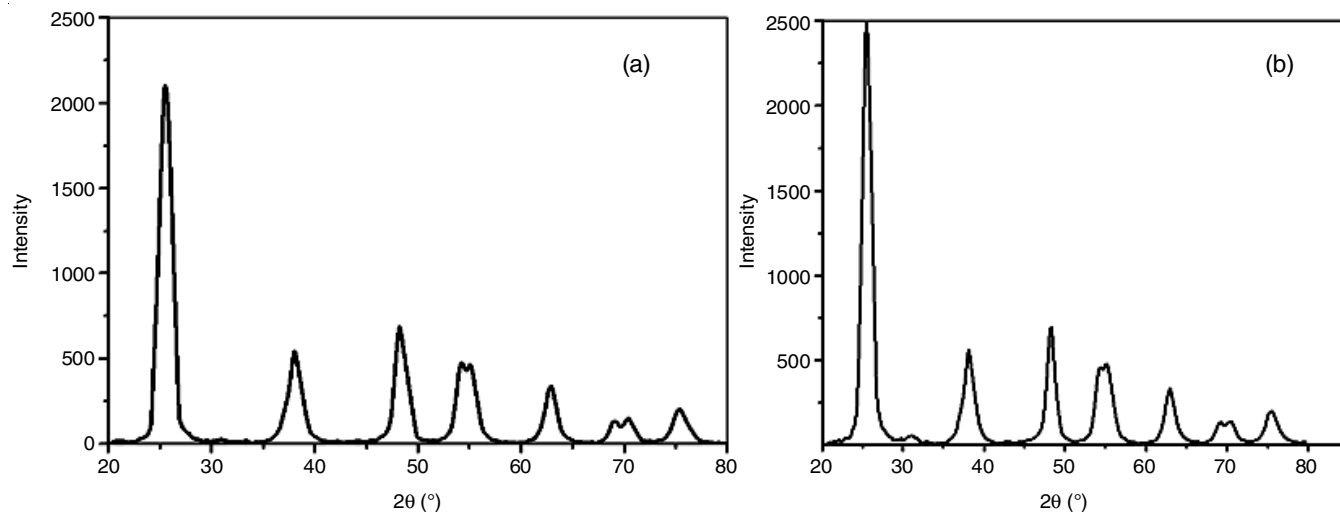

Fig. 1. XRD spectra of (a) GT1 and (b) T1

allite size of GT1 nanocomposite was comparatively lower than that of T1 confirmed the incorporation of graphene in titania system. The peak width of GT1 is slightly broadened than T1, which may be also due to the graphene-titania interaction [57].

FTIR analysis: Fig. 2a-b represents the FTIR spectra of GT1 and T1, respectively. A broad band was obtained around 500-700 cm^{-1} and 3400-3420 cm^{-1} which may be, respectively due to the Ti–O–Ti stretching and O–H stretching vibrations. A board peak at 1625 cm^{-1} represents a hydroxyl group [6] and also some low intensity peaks were seen due to the stretching vibrations [5,6,18,58].
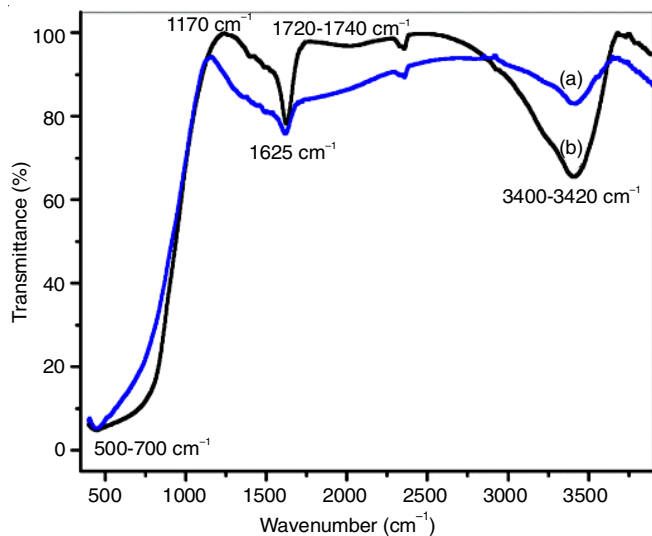

Fig. 2. FTIR spectra of (a) AT1 and (b) T1

UV-visible diffuse reflectance spectra: The UV-visible diffuse reflectance spectra of GT1 and T1 are shown in Fig. 3a-b, respectively. For GT1 nanocomposite, the absorption edge is extended more to visible region. Such a shift may be due to the Ti-O-C bond [18,59,60].
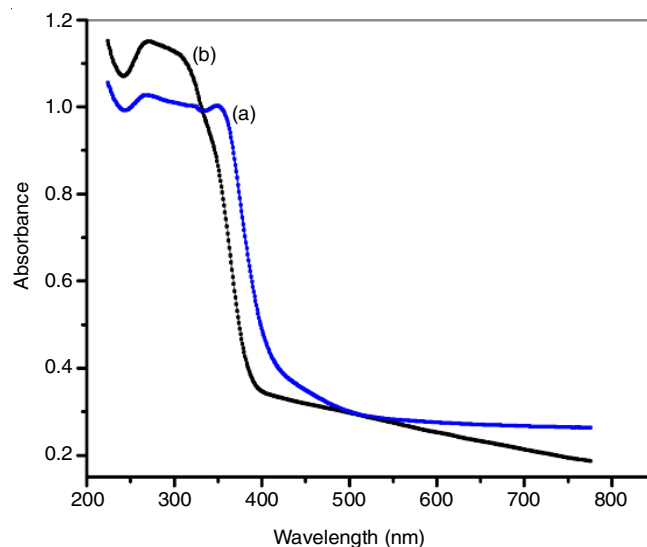

Fig. 3. UV-visible spectra of (a) GT1 and (b) T1

TEM analysis: TEM images in Fig. 4a-b clearly depicts the distribution of titania nanoparticles on graphene sheets. Titania particles with 7-13 nm size have spherical morphology even though some portions have agglomerization. Graphene sheets as clearly seen in Fig. 4b. HRTEM and SAED images
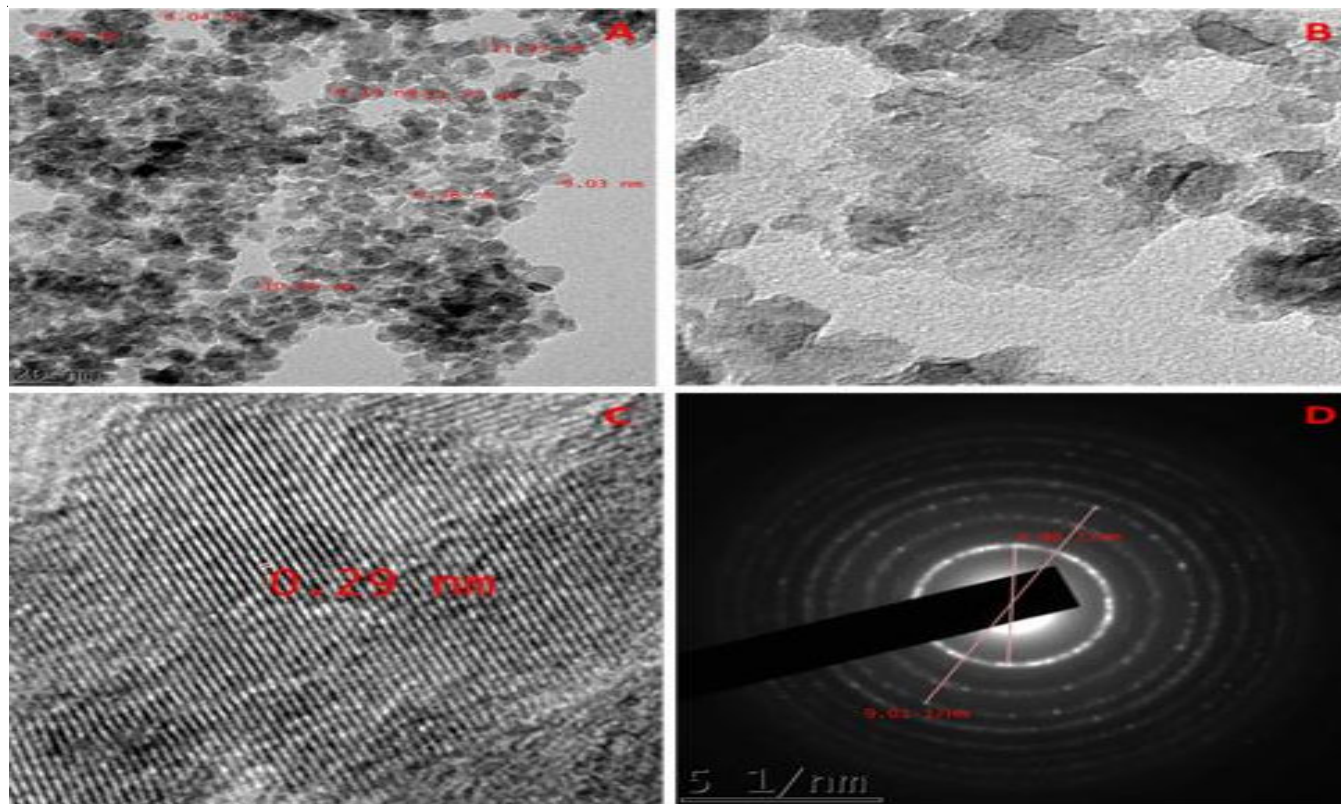

Fig. 4. (a,b) TEM images, (c) indicates HRTEM image and (d) demonstrates SAED images of GT1
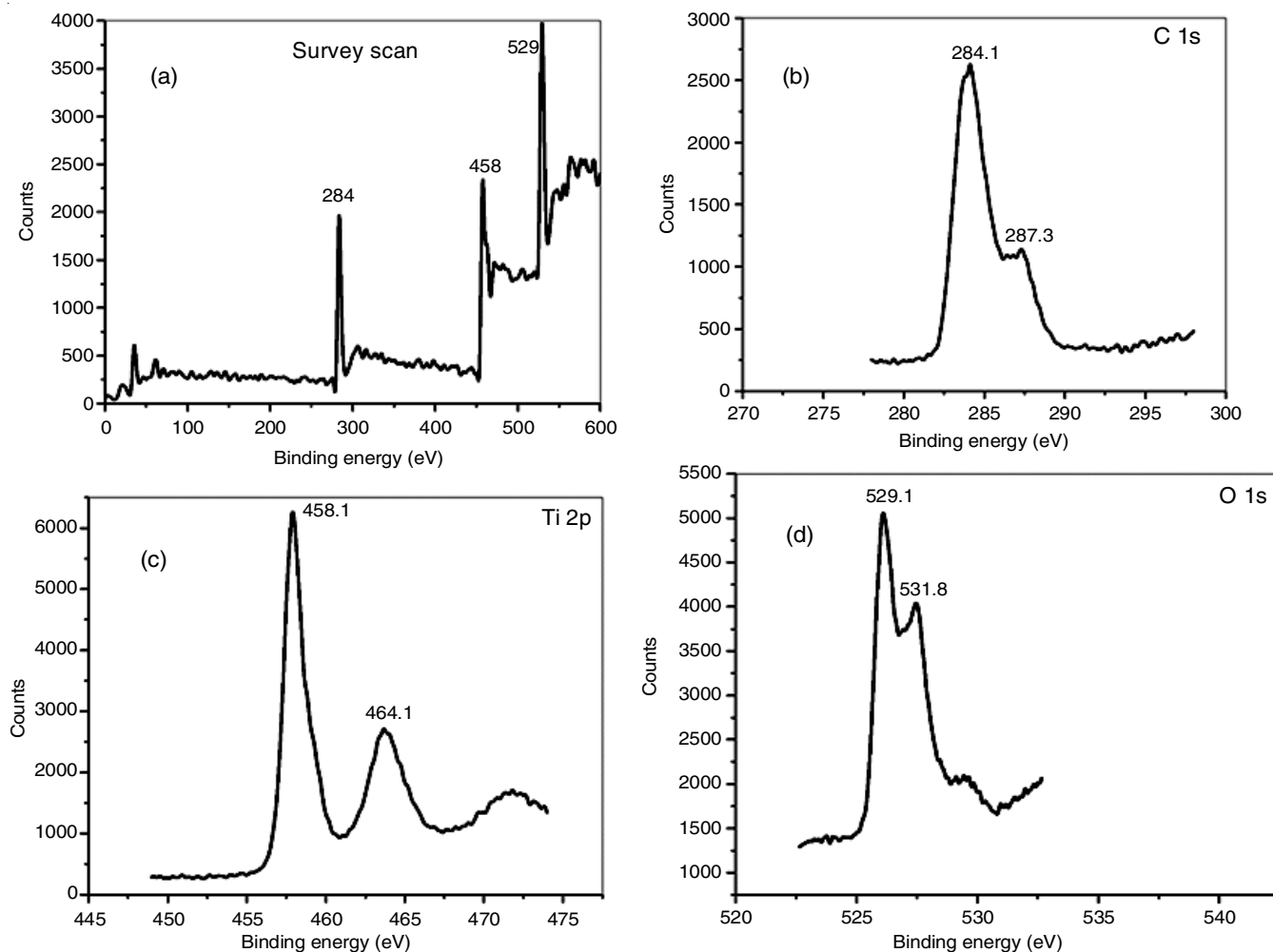
Fig. 5. (a) Survey scan, (b) carbon 1s, (c) carbon shows titanium 2p and (d) oxygen 1s XPS spectra of GT1

in Fig. 4c-d shows the crystalline and ordered morphology of GT1 nanoparticles, which also supports XRD results.

XPS analysis: Fig. 5a depicts XPS survey scan spectra and Fig. 5b shows carbon 1s peak. Two peaks near 284.1 eV and 287.2 eV provided in Fig. 5b arises due to elemental carbon and due to the presence of a carbonate species, respectively [10,20,29,60-62]. Two peaks were obtained at binding energies 458.1 eV and 464.1 eV that corresponds to 2p3/2 and 2p1/2 states of titanium (Fig. 5c). A peak at 529.1 eV for oxygen 1s level (Fig. 5d) is due to oxygen in Ti-O network and the peak near 531.8 eV, which may be due to the presence of oxygen in the hydroxyl group [10]. Thus, all the elements present in GT1 composite were confirmed.

Photocatalytic activity

Effect of amount of catalyst: Fig. 6 represents the percentage degradation of methylene blue dye by GT1 catalyst. It was observed that the degradation of methylene blue dye increases with increasing amount of GT1 and attained an optimum value of about 90% at 3 g/L of GT1. This could be due to the availability of more active sites on the surface of the catalyst, allowing it to absorb more light. However, once the optimal value limit was exceeded, only insignificant increase in degradation was observed.
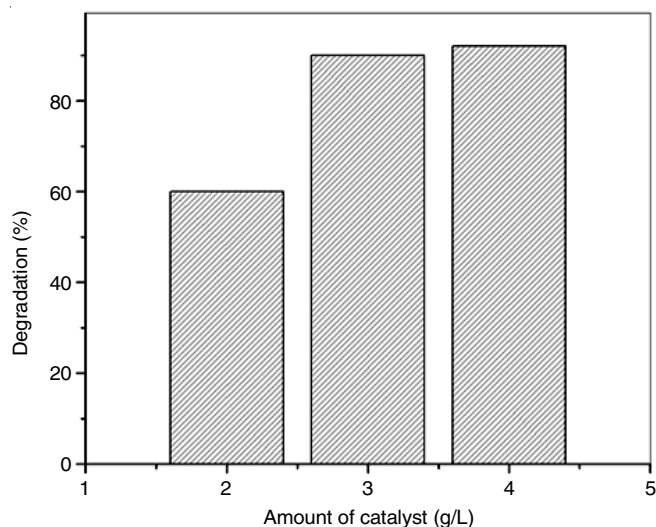

Fig. 6. Percentage degradation of methylene blue dye against amount of GT1

Effect of time: The study involved about 50 mL of 10^{-4} M aqueous solution of methylene blue dye with GT1 of 3 g/L added and irradiated for 0.5 h to attain an equilibrium between methylene blue dye molecules and the GT1 surface. After irradiating the system under sunlight, 10 mL was pipetted at

regular intervals and the absorbance was measured. Also there is a linear increase in percentage of degradation with increasing time (Fig. 7). With increase in time, more light can fall on the catalyst surface that may increase the excited species formation thereby enhancing the photocatalytic efficiency.
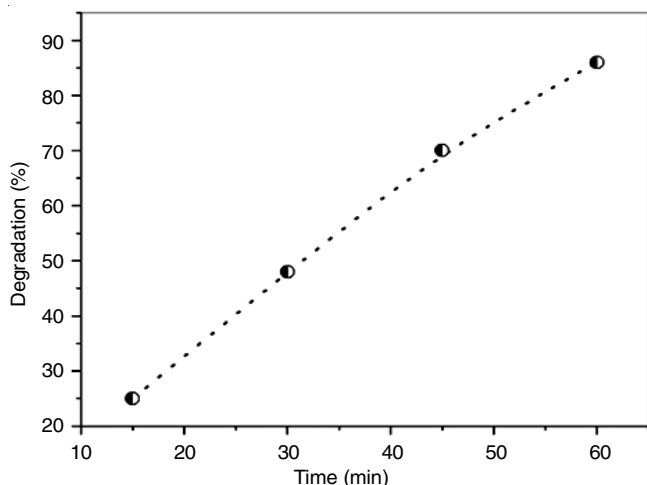
Effect of catalysts: The percentage degradation of methylene blue dye was carried out by GT1 and pure T1 under the same concentration and irradiation time. As observed in Table-1, the higher degradation percentage was obtained for GT1 than pure T1 indicating the impact of graphene incorporation.

Fig. 7. Percentage degradation of methylene blue dye against solar irradiation

TABLE-1
PERCENTAGE DEGRADATION OF
METHYLENE BLUE AGAINST CATALYST

Catalyst	Degradation (%)
G-TiO$_2$	90
TiO$_2$	40

Time under sunlight: 60 min; MBD conc.: 10 mL of 10^{-4} M, GT1 amount: 3 g/L

Moreover, Table-2 represents a comparison degradation efficiency of methylene blue dye incorporated binary and ternary composites prepared by different methods. Most of the composites mentioned in Table-2 were prepared by hydrothermal method and showed different efficiency of degradation. Thus, it is clearly indicated that binary GT1 nanocomposite has a comparatively higher effectiveness in the photocatalytic break-down of methylene blue dye.

TABLE-2
COMPARISON CHART OF MBD1 DEGRADATION OF GRAPHENE INCORPORATED TITANIA BY VARIOUS METHODS

Sl. No.	Catalyst name	Dye conc. (mg/mL)	Catalyst conc. (mg/mL)	Time (min)	Degradation (%)	Methods	Ref.	Remarks
1	Graphene-TiO$_2$ (GT1) nanocomposite	3.74×10^{-5}	3	60	Above 90	Sol-gel	Present work	
2	TiO$_2$/graphene/Ag	1.0×10^{-2}	1.0	60	80-85	Sol-gel	[63]	Incorporation of Ag nanoparticles
3	GO/TiO$_2$	6×10^{-2}	1	150	20	Sol-gel	[64]	UV light irradiation
4	TiO$_2$/SiO$_2$/-Fe$_2$O$_3$/rGO	3.74×10^{-6}	0.25	30	66	Sol-gel	[65]	Incorporation of SiO$_2$ and Fe$_2$O$_3$
5	P25-graphene	10.3×10^{-6}	0.75	60	65	Hydrothermal	[66]	
6	CSA/TiO$_2$/rGO	5×10^{-3}	0.1	30	Above 90	Hydrothermal	[26]	UV light
7	TNTS/rGO	2×10-2	0.25	60	60	Hydrothermal	[67]	
8	Graphene-supported TiO$_2$			60	Above 90	Hydrothermal	[68]	
9	P25–graphene (GN)	1×10^{-2}	0.4	60	80-90	Hydrothermal	[69]	UV
10	TiO$_2$/GO.	3.74×10^{-6}	1	60	55%	Hydrothermal	[70]	
11	Graphene/titania (GR/TiO2)	2×10^{-2}	1			Hydrothermal	[71]	UV
12	TiO$_2$/diazonium/graphene oxide	1×10^{-4}	0.2	120	67	Hydrothermal	[72]	
13	GO@TiO$_2$-500	1×10^{-7}	0.62	60	90	Thermal annealing treatment	[73]	
14	TiO$_2$/reduced graphene oxide	1×10^{-2}	0.8	90	Above 90	Two-step hydrothermal and calcinations synthesis	[74]	UV-visible
15	RGO/TiO$_2$ composites	1×10^{-2}	0.5	60	Above 90	Sonication	[75]	UV
16	MgFe$_2$O$_4$–TiO$_2$NPs@GO	0.5	0.5	120	Above 90	Ultrasonication	[76]	
17	Graphene@TiO$_2$	1×10^{-2}	0.5	180	85	Sonication and Solvothermal	[77]	
18	Graphene/TiO$_2$	7.4×10^{-6}	0.3	60	35	One-step solvothermal method	[78]	

19	rGO/TiO$_2$	1×10^{-1}	0.5	60	Above 90	Ultrasonic spray pyrolysis	[79]	UV
20	TiO$_2$/graphene oxide	9.35×10^{-6}	0.2	60	80-90	One-step colloidal blending and Sonication	[55]	High content of graphene
21	Nitrogen-doped reduced graphene oxide (N-RGO)	7.4×10^{-6}	0.5	160	80	Annealing	[80]	
22	TiO$_2$ nanoparticles loaded on graphene/carbon composite nanofibers (TiO$_2$-CCNF).	15×10^{-8}	1.0	30	Above 90	Electro-spinning techniques	[81]	
23	RGO/TiO$_2$	1×10^{-2}	0.8	30	20	Electrophoretic	[82]	
24	RGO/TiO$_2$ composites	1.87×10^{-5}	0.4	60	Above 90	*In situ* redox method	[83]	
25	TiO$_2$/Graphene oxide	5×10^{-3}	0.5	45	Above 90	Liquid phase deposition	[43]	
26	TiO$_2$ (P25)-graphene composite hydrogels	1×10^{-2}	0.75	60	Above 90	Self assembled gelation method	[84]	
27	RGO/TiO$_2$	7.48×10^{-6}	1.0	60	90	Facile mechanical method	[85]	

Conclusion

A nanocrystalline graphene-TiO$_2$ (GT1) nanocomposite was successfully prepared through modified sol gel method. The XRD results confirmed that nanocrystalline graphene-TiO$_2$ (GT1) nanocomposite have pure anatase phase. IR spectrum indicates the presence of carbon and the XPS analysis confirms the presence of all elements present in GT1 nanocomposite. Also, more than 90% degradation of methylene blue dye on irradiation under sunlight with optimum GT1 nanocomposite amount of 3 g/L was achieved within 1 h.

CONFLICT OF INTEREST

The authors declare that there is noconflict of interests regarding the publication of this article.

REFERENCES

1. N. Morin-Crini, E. Lichtfouse, G. Liu, V. Balaram, A.R.L. Ribeiro, Z. Lu, F. Stock, E. Carmona, M.R. Teixeira, L.A. Picos-Corrales, J.C. Moreno-Piraján, L. Giraldo, C. Li, A. Pandey, D. Hocquet, G. Torri and G. Crini, *Environ. Chem. Lett.*, **20**, 2311 (2022); https://doi.org/10.1007/s10311-022-01447-4
2. M.T.H. Van Vliet, E.R. Jones, M. Florke, W.H.P. Franssen, N. Hanasaki, Y. Wada and J.R. Yearsley, *Environ. Res. Lett.*, **16**, 024020 (2021); https://doi.org/10.1088/1748-9326/abbfc3
3. P. Shandilya, P. Raizada and P. Singh, *Photocatalysis*, **57**, 119 (2021); https://doi.org/10.1007/978-3-030-54723-3
4. N. Bhattacharjee, I. Som, R. Saha and S. Mondal, *Int. J. Environ. Anal. Chem.*, (2022); https://doi.org/10.1080/03067319.2021.2022130
5. S. Khanna, P. Marathey, S. Paneliya, P. Vinchhi, R. Chaudhari and J. Vora, *Int. J. Hydrogen Energy*, **47**, 41698 (2022); https://doi.org/10.1016/j.ijhydene.2022.02.050
6. P. Muthirulan, C. Nirmala Devi and M. Meenakshi Sundaram, *Mater. Sci. Semicond. Process.*, **25**, 219 (2014); https://doi.org/10.1016/j.mssp.2013.11.036
7. B.Y.S. Chang, N.M. Huang, M. Nor An'amt, A.R. Marlinda, Y. Norazriena, M.R. Muhamad, I. Harrison, H.N. Lim and C.C. Hua, *Int. J. Nanomedicine*, **2012**, 3379 (2012); https://doi.org/10.2147/IJN.S28189
8. J.P. Jeon, D.H. Kweon, B.J. Jang, M.J. Ju and J.B. Baek, *Adv. Sustain. Syst.*, **4**, 2000197 (2020); https://doi.org/10.1002/adsu.202000197
9. R. Nawaz, C.F. Kait, H.Y. Chia, M.H. Isa and L.W. Huei, *Environ. Technol. Innov.*, **19**, 101007 (2020); https://doi.org/10.1016/j.eti.2020.101007
10. N.R. Khalid, E. Ahmed, Z. Hong, L. Sana and M. Ahmed, *Curr. Appl. Phys.*, **13**, 659 (2013); https://doi.org/10.1016/j.cap.2012.11.003
11. V. Stengl, S. Bakardjieva and N. Murafa, *Mater. Chem. Phys.*, **114**, 217 (2009); https://doi.org/10.1016/j.matchemphys.2008.09.025
12. R. Asahi, T. Morikawa, T. Ohwaki, K. Aoki and Y. Taga, *Science*, **293**, 269 (2001); https://doi.org/10.1126/science.1061051
13. J.M. Herrmann, *Catal. Today*, **53**, 115 (1999); https://doi.org/10.1016/S0920-5861(99)00107-8
14. J. Wang, D.N. Tafen, J.P. Lewis, Z. Hong, A. Manivannan, M. Zhi, M. Li and N. Wu, *J. Am. Chem. Soc.*, **131**, 12290 (2009); https://doi.org/10.1021/ja903781h
15. D.N. Tafen, J. Wang, N.Q. Wu and J.P. Lewis, *Appl. Phys. Lett.*, **94**, 093101 (2009); https://doi.org/10.1063/1.3093820
16. S. Kohtani, S. Makino, A. Kudo, K. Tokumura, Y. Ishigaki, T. Matsunaga, O. Nikaido, K. Hayakawa and R. Nakagaki, *Chem. Lett.*, **31**, 660 (2002); https://doi.org/10.1246/cl.2002.660
17. Y. Yu, J.C. Yu, C.Y. Chan, Y.K. Che, J.C. Zhao, L. Ding, W.K. Ge and P.K. Wong, *Appl. Catal. B*, **61**, 1 (2005); https://doi.org/10.1016/j.apcatb.2005.03.008
18. X. Liu, Y. Yang, H. Li, Z. Yang and Y. Fang, *Chem. Eng. J.*, **408**, 127259 (2021); https://doi.org/10.1016/j.cej.2020.127259
19. S. Ali, A. Razzaq and S.-I. In, *Catal. Today*, **335**, 39 (2019); https://doi.org/10.1016/j.cattod.2018.12.003
20. X.-Y. Zhang, H.-P. Li, X.-L. Cui and Y. Lin, *J. Mater. Chem.*, **20**, 2801 (2010); https://doi.org/10.1039/b917240h
21. M.Q. Yang, N. Zhang and Y.J. Xu, *ACS Appl. Mater. Interfaces*, **5**, 1156 (2013); https://doi.org/10.1021/am3029798
22. K.S. Novoselov, A.K. Geim, S.V. Morozov, D. Jiang, Y. Zhang, S.V. Dubonos, I.V. Grigorieva and A.A. Firsov, *Science*, **306**, 666 (2004); https://doi.org/10.1126/science.1102896
23. A.K. Geim and K.S. Novoselov, *Nat. Mater.*, **6**, 183 (2007); https://doi.org/10.1038/nmat1849
24. S. Stankovich, D.A. Dikin, R.D. Piner, K.A. Kohlhaas, A. Kleinhammes, Y. Jia, Y. Wu, S.T. Nguyen and R.S. Ruoff, *Carbon*, **45**, 1558 (2007); https://doi.org/10.1016/j.carbon.2007.02.034
25. S. Linley, Y.Y. Liu, C.J. Ptacek, D.W. Blowes and F.X. Gu, *ACS Appl. Mater. Interfaces*, **6**, 4658 (2014); https://doi.org/10.1021/am4039272

26. Z. Wang, M. Zhang, Z. Song, M. Yaseen, Z. Huang, A. Wang, Z. Guisheng and S. Shao, *J. Colloid Interface Sci.*, **624**, 88 (2022); https://doi.org/10.1016/j.jcis.2022.05.094

27. I. Khan, K. Saeed, I. Zekker, B. Zhang, A.H. Hendi, A. Ahmad, S. Ahmad, N. Zada, H. Ahmad, L.A. Shah, T. Shah and I. Khan, *Water*, **14**, 242 (2022); https://doi.org/10.3390/w14020242

28. S.A. Kidd, P.A. Lancaster, J.C. Anderson, A. Boogert, C.C.Fisher, R. Robertson and D.M. Wass, *Prenat. Diagn.*, **16**, 39 (1996); https://doi.org/10.1002/(SICI)1097-0223(199601)16:1<39::AID-PD789>3.0.CO;2-P

29. G. Rajivgandhi, V. Rtv, R. Nandhakumar, S. Murugan, N.S. Alharbi, S. Kadaikunnan, J.M. Khaled, K.F. Alanzi and W.-J. Li, *Environ. Res.*, **199**, 111322 (2021); https://doi.org/10.1016/j.envres.2021.111322

30. R. Suresh, L. Gnanasekaran, S. Rajendran, M. Soto-Moscoso, W.-H. Chen, P.L. Show and K.S. Khoo, *Environ. Technol. Innov.*, **31**, 103149 (2023); https://doi.org/10.1016/j.eti.2023.103149

31. Y. Hua, S. Wang, J. Xiao, C. Cui and C. Wang, *RSC Adv.*, **7**, 28979 (2017); https://doi.org/10.1039/C6RA23939K

32. A. Pruna, Q. Shao, M. Kamruzzaman, Y.Y. Li, J.A. Zapien, D. Pullini, D. Busquets Mataix and A. Ruotolo, *Appl. Surf. Sci.*, **392**, 801 (2017); https://doi.org/10.1016/j.apsusc.2016.09.122

33. R. Atchudan, T.N.J.I. Edison, S. Perumal, M. Shanmugam and Y.R. Lee, *J. Photochem. Photobiol. Chem.*, **337**, 100 (2017); https://doi.org/10.1016/j.jphotochem.2017.01.021

34. A. Pruna, Z. Wu, J. Zapien, Y. Li and A. Ruotolo, *Appl. Surf. Sci.*, **441**, 936 (2018); https://doi.org/10.1016/j.apsusc.2018.02.117

35. H. Wang, Q. Shen, Z. You, Y. Su, Y. Yu, A. Babapour, F. Zhang, D. Cheng and H. Yang, *Mater. Lett.*, **217**, 143 (2018); https://doi.org/10.1016/j.matlet.2018.01.037

36. H. Zhou, X. Yue, H. Lv, L. Kong, Z. Ji and X. Shen, *Ceram. Int.*, **44**, 7240 (2018); https://doi.org/10.1016/j.ceramint.2018.01.176

37. B.K. Choi, W.K. Choi, S.J. Park and M.K. Seo, *J. Nanosci. Nanotechnol.*, **18**, 6075 (2018); https://doi.org/10.1166/jnn.2018.15616

38. M.R.U.D. Biswas, B.S. Ho and W.C. Oh, *Polym. Bull.*, **77**, 4381 (2020); https://doi.org/10.1007/s00289-019-02973-y

39. I. Ali, S.R. Kim, K. Park and J.O. Kim, *Opt. Mater. Express*, **7**, 1535 (2017); https://doi.org/10.1364/OME.7.001535

40. A. Datcu, M. Mendoza, A.P. del Pino, C. Logofatu, C. Luculescu and E. György, *Catal. Today*, **321-322**, 81 (2019); https://doi.org/10.1016/j.cattod.2018.02.026

41. R. Atchudan, T.N.J. Immanuel Edison, S. Perumal, D. Karthikeyan and Y.R. Lee, *J. Photochem. Photobiol. Chem.*, **333**, 92 (2017); https://doi.org/10.1016/j.jphotochem.2016.10.021

42. J. Ahmad, F.A. Sofi, O. Mehraj and K. Majid, *Surf. Interfaces*, **13**, 186 (2018); https://doi.org/10.1016/j.surfin.2018.09.010

43. S.A. Khan, Z. Arshad, S. Shahid, I. Arshad, K. Rizwan, M. Sher and U. Fatima, *Compos., Part B Eng.*, **175**, 107120 (2019); https://doi.org/10.1016/j.compositesb.2019.107120

44. S. Gupta Chatterjee, S. Chatterjee, A.K. Ray and A.K. Chakraborty, *Sens. Actuators B Chem.*, **221**, 1170 (2015); https://doi.org/10.1016/j.snb.2015.07.070

45. Y. Liang, H. Wang, H. Sanchez Casalongue, Z. Chen and H. Dai, *Nano Res.*, **3**, 701 (2010); https://doi.org/10.1007/s12274-010-0033-5

46. C. Chen, W. Cai, M. Long, B. Zhou, Y. Wu, D. Wu and Y. Feng, *ACS Nano*, **4**, 6425 (2010); https://doi.org/10.1021/nn102130m

47. R. Lakra, R. Kumar, P.K. Sahoo, D. Thatoi and A. Soam, *Inorg. Chem. Commun.*, **133**, 108929 (2021); https://doi.org/10.1016/j.inoche.2021.108929

48. G. Williams, B. Seger and P.V. Kamat, *ACS Nano*, **2**, 1487 (2008); https://doi.org/10.1021/nn800251f

49. P. Wang, Y.M. Zhai, D.J. Wang and S.J. Dong, *Nanoscale*, **3**, 1640 (2011); https://doi.org/10.1039/c0nr00714e

50. C.C. Wang and J.Y. Ying, *Chem. Mater.*, **11**, 3113 (1999); https://doi.org/10.1021/cm990180f

51. M. Keshmiri, M. Mohseni and T. Troczynski, *Appl. Catal. B*, **53**, 209 (2004); https://doi.org/10.1016/j.apcatb.2004.05.016

52. W.S. Hummers Jr. and R.E. Offeman, *J. Am. Chem. Soc.*, **80**, 1339 (1958); https://doi.org/10.1021/ja01539a017

53. J.Y. Jang, M.S. Kim, H.M. Jeong and C.M. Shin, *Compos. Sci. Technol.*, **69**, 186 (2009); https://doi.org/10.1016/j.compscitech.2008.09.039

54. G. Jiang, X. Zheng, Y. Wang, T. Li and X. Sun, *Powder Technol.*, **207**, 465 (2011); https://doi.org/10.1016/j.powtec.2010.11.029

55. T.D. Nguyen-Phan, V.H. Pham, E.W. Shin, H.D. Pham, S. Kim, J.S. Chung, E.J. Kim and S.H. Hur, *Chem. Eng. J.*, **170**, 226 (2011); https://doi.org/10.1016/j.cej.2011.03.060

56. W. Fan, Q. Lai, Q. Zhang and Y. Wang, *J. Phys. Chem. C*, **115**, 10694 (2011); https://doi.org/10.1021/jp2008804

57. Y. Zhang, Z.R. Tang, X. Fu and Y.J. Xu, *ACS Nano*, **5**, 7426 (2011); https://doi.org/10.1021/nn202519j

58. D.C. Marcano, D.V. Kosynkin, J.M. Berlin, A. Sinitskii, A. Slesarev, Z. Sun, L.B. Alemany, W. Lu and J.M. Tour, *ACS Nano*, **4**, 4806 (2010); https://doi.org/10.1021/nn1006368

59. G. Jiang, Z. Lin, C. Chen, L. Zhu, Q. Chang, N. Wang, W. Wei and H. Tang, *Carbon*, **49**, 2693 (2011); https://doi.org/10.1016/j.carbon.2011.02.059

60. S. Sakthivel and H. Kisch, *Angew. Chem. Int. Ed.*, **42**, 4908 (2003); https://doi.org/10.1002/anie.200351577

61. X.G. Gao, L.X. Cheng, W.S. Jiang, X.K. Li and F. Xing, *Front Chem.*, **9**, 615164 (2021); https://doi.org/10.3389/fchem.2021.615164

62. N. Serpone, *J. Phys. Chem. B*, **110**, 24287 (2006); https://doi.org/10.1021/jp065659r

63. Y.Y. Wen, H.M. Ding and Y.K. Shan, *Nanoscale*, **3**, 4411 (2011); https://doi.org/10.1039/c1nr10604j

64. Z. Fu, S. Zhang and Z. Fu, *Appl. Sci.*, **9**, 3282 (2019); https://doi.org/10.3390/app9163282

65. R. Kaveh, M. Mokhtarifar, M. Bagherzadeh, A. Lucotti, M.V. Diamanti and M.P. Pedeferri, *Molecules*, **25**, 2996 (2020); https://doi.org/10.3390/molecules25132996

66. H. Zhang, X. Lv, Y. Li, Y. Wang and J. Li, *ACS Nano*, **4**, 380 (2010); https://doi.org/10.1021/nn901221k

67. X. Niu, W. Yan, H. Zhao and J. Yang, *Appl. Surf. Sci.*, **440**, 804 (2018); https://doi.org/10.1016/j.apsusc.2018.01.069

68. N. Singh, S. Jana, G.P. Singh and R.K. Dey, *Adv. Compos. Hybrid Mater.*, **3**, 127 (2020); https://doi.org/10.1007/s42114-020-00140-w

69. J. Li, S. Zhou, G.-B. Hong and C.-T. Chang, *Chem. Eng. J.*, **219**, 486 (2013); https://doi.org/10.1016/j.cej.2013.01.031

70. R.T. Yunarti, T.N. Safitri, L.C.C. Dimonti, G. Aulia, M. Khalil and M. Ridwan, *J. Phys. Chem. Solids*, **160**, 110357 (2022); https://doi.org/10.1016/j.jpcs.2021.110357

71. X. Wang, S. Han, Q. Zhang, N. Zhang and D. Zhao, *MATEC Web of Conf.*, **238**, 03006 (2018); https://doi.org/10.1051/matecconf/201823803006

72. N.T.V. Hoan, N.N. Minh, T.T.K. Nhi, N. Van Thang, V.A. Tuan, V.T. Nguyen, N.M. Thanh, N. Van Hung and D.Q. Khieu, *J. Nanomater.*, **2020**, 1 (2020); https://doi.org/10.1155/2020/4350125

73. F.-E. Zirar, A. Anouar, N. Katir, I.A. Ichou and A. El Kadib, *RSC Advances*, **11**, 28116 (2021); https://doi.org/10.1039/D1RA05275F

74. E.K. Nejman, A. Wanag, J. Kapica-Kozar, L. Kowalczyk, B. Tryba, M. Zgrzebnicki, J. Przepiórski and A.W. Morawski, *Catal. Today*, **357**, 630 (2020); https://doi.org/10.1016/j.cattod.2019.04.078

75. V. Loryuenyong, J. Charoensuk, R. Charupongtawitch, A. Usakulwattana and A. Buasri, *J. Nanosci. Nanotechnol.*, **16**, 296 (2016);
https://doi.org/10.1166/jnn.2016.11612

76. J. Kaur and M. Kaur, *Ceram. Int.*, **45**, 8646 (2019);
https://doi.org/10.1016/j.ceramint.2019.01.185

77. D. Zhao, G. Sheng, C. Chen and X. Wang, *Appl. Catal. B*, **111-112**, 303 (2012);
https://doi.org/10.1016/j.apcatb.2011.10.012

78. Y. Min, K. Zhang, W. Zhao, F.C. Zheng, Y.C. Chen and Y.G. Zhang, *Chem. Eng. J.*, **193-194**, 203 (2012);
https://doi.org/10.1016/j.cej.2012.04.047

79. J.A. Park, B. Yang, J. Lee, I.G. Kim, J.H. Kim, J.W. Choi, H.D. Park, I.W. Nah and S.H. Lee, *Chemosphere*, **191**, 738 (2018);
https://doi.org/10.1016/j.chemosphere.2017.10.094

80. X. Yin, H. Zhang, P. Xu, J. Han, J. Li and M. He, *RSC Adv.*, **3**, 18474 (2013);
https://doi.org/10.1039/c3ra43403f

81. C.H. Kim, B. Kim and K.S. Yang, *Carbon*, **50**, 2472 (2012);
https://doi.org/10.1016/j.carbon.2012.01.069

82. E. Noormohammadi and S. Sanjabi, *Surf. Rev. Lett.*, **27**, 9 (2019);
https://doi.org/10.1142/S0218625X19501117

83. R.K. Nainani and P. Thakur, *Water Sci. Technol.*, **73**, 1927 (2016);
https://doi.org/10.2166/wst.2016.039

84. C. Hou, Q. Zhang, Y. Li and H. Wang, *J. Hazard. Mater.*, **205-206**, 229 (2012);
https://doi.org/10.1016/j.jhazmat.2011.12.071

85. M.A.E. Wafi, M.A. Ahmed, H.S. Abdel-Samad and H.A.A. Medien, *Mater. Sci. Energy Technol.*, **5**, 217 (2022);
https://doi.org/10.1016/j.mset.2022.02.003